

1 Experimental Determination of Solubilities of Sodium Tetraborate (Borax) in NaCl
2 Solutions, and A Thermodynamic Model for the Na–B(OH)₃–Cl–SO₄ System to High
3 Ionic Strengths at 25 °C, Revision 1 Corrections

4

5 Yongliang Xiong¹, Leslie Kirkes, and Terry Westfall

6 Sandia National Laboratories (SNL)*
7 Carlsbad Programs Group
8 4100 National Parks Highway, Carlsbad, NM 88220, USA

9

¹ Corresponding author, e-mail: yxiong@sandia.gov.

* Sandia is a multiprogram laboratory operated by Sandia Corporation, a wholly owned subsidiary of Lockheed Martin Corporation, for the United States Department of Energy's National Nuclear Security Administration under contract DE-AC04-94AL85000.

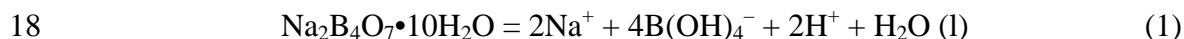
This research is funded by WIPP programs administered by the Office of Environmental Management (EM) of the U.S Department of Energy.

10

11 ABSTRACT

12 In this study, solubility experiments on sodium tetraborate ($\text{NaB}_4\text{O}_7 \cdot 10\text{H}_2\text{O}$,
13 borax) are conducted in NaCl solutions up to 5.0 m at room temperature ($22.5 \pm 1.5^\circ\text{C}$).
14 In combination with solubility data of sodium tetraborate in Na_2SO_4 solutions from
15 literature, the solubility constant ($\log K_{sp}$) for sodium tetraborate for the following
16 reaction,

17



19

20 is determined as -24.80 ± 0.10 based on the Pitzer model. In conjunction with the
21 relevant Pitzer parameters, based on the above $\log K_{sp}$ for borax, and $\log \beta_I$ (0.25 ± 0.01)
22 evaluated from the literature for the following complex formation reaction,

23



25

26 a thermodynamic model with high precision is established for the $\text{Na}^+ - \text{B}(\text{OH})_3 - \text{Cl}^- -$
27 SO_4^{2-} system at high ionic strengths up to saturation of halite (NaCl), mirabilite
28 ($\text{Na}_2\text{SO}_4 \cdot 10\text{H}_2\text{O}$) and thenardite (Na_2SO_4). The model is validated by comparison of
29 model predicted equilibrium compositions for the assemblages of borax alone, borax +
30 halite, borax + mirabilite, borax + halite + thenardite, and borax + mirabilite + thenardite
31 in the mixtures of NaCl + Na_2SO_4 to ionic strengths of 8.0 m, with independent
32 experimental values from the literature. The differences in concentrations of major ions,

33 e.g., Na^+ , Cl^- , and SO_4^{2-} , between model predicted and experimental values are generally
34 less than 0.5%. The difference for total boron concentrations is less than 0.05 m with an
35 error less than 25%.

36 The revised thermodynamic model is applied to the potential recovery of borax
37 from boron-enriched brines via evaporation at 25°C, using the two brines from China as
38 examples. The reaction path calculations suggest that the brine from the Zhabei Salt
39 Lake in Xizang (Tibet) Autonomous Region, is suitable to recovery of borax via
40 evaporation at 25°C, whereas the brine from the western Sichuan Province, although it is
41 enriched in boron, is not suitable to extraction of boron as borax, but is suitable to
42 extraction of potassium as sylvite, via evaporation at 25°C.

43

44 INTRODUCTION

45 Numerous actinide borates have been recently successfully synthesized (e.g.,
46 Wang et al., 2010, 2011, and references therein), including a Pu(III) borate,
47 $\text{Pu}_2[\text{B}_{12}\text{O}_{18}(\text{OH})_4\text{Br}_2(\text{H}_2\text{O})_3]\cdot 0.5\text{H}_2\text{O}$. Furthermore, a recent experimental study has
48 suggested that borate could potentially complex with Nd(III), an analog to Am(III)
49 (Borkowski et al., 2010). Therefore, a comprehensive thermodynamic model involving
50 interactions of borate with major ions in brines is needed to accurately describe the
51 contributions of borate to the solubility of Am(III) in brines in salt formations, as they
52 contain significant concentrations of borate. In brines associated with salt formations,
53 they contain high concentrations of sodium along with significant concentrations of
54 boron. For instance, at the Waste Isolation Pilot Plant (WIPP), a U.S. Department of
55 Energy geological repository for the permanent disposal of defense-related transuranic

56 (TRU) waste (U.S. DOE, 1996), the Generic Weep Brine (GWB) and Energy Research
57 and Development Administration Well 6 (ERDA-6), contain high concentrations of
58 sodium and borate. Therefore, in geological repositories in salt formations, the
59 interactions between sodium and borate will be important to the accurate description of
60 the contributions of borate to the solubility of Am(III) in brines in salt formations.

61 A thermodynamic model for borate at high ionic strengths was developed more
62 than two decades ago by Felmy and Weare (1986). In addition to the newly generated
63 data at Sandia National Laboratories, there have also been numerous experimental data
64 concerning borate in concentrated brines generated in China (e.g., Sang et al., 2011),
65 since the discovery of enormous amounts of highly concentrated brines with high
66 concentrations of B (up to 4994 mg/L) and Li (up to 90 mg/L), termed as “liquid ores”, in
67 Sichuan Province, China (e.g., Lin et al., 2000). Therefore, in light of new experimental
68 data, the revision of the Felmy and Weare model is in order. There will be a series of
69 upcoming publications in this area, and this paper is the first one in this series.

70

71 EXPERIMENTAL METHODS

72

73 In our solubility experiments, about 5 grams of the solubility controlling
74 material—ACS reagent grade sodium tetraborate ($\text{Na}_2\text{B}_4\text{O}_7 \cdot 10\text{H}_2\text{O}$), i.e., borax, from
75 Fisher Scientific was weighed out and placed into 150 mL plastic bottles. Then, 100 mL
76 of supporting solutions were added into those bottles. Once filled, the lids of the bottles
77 were sealed with parafilm. The supporting electrolytes are a series of NaCl solutions
78 ranging from 0.010 m to 5.0 m. Undersaturation experiments are conducted at the
79 laboratory room temperature ($22.5 \pm 1.5^\circ\text{C}$), and the duration of our experiments is

80 exceedingly long in comparison with the similar studies previously conducted (see
81 RESULTS section). In the following, sodium tetraborate and borax will be
82 interchangeably used.

83 The pH readings were measured with an Orion-Ross combination pH glass
84 electrode, coupled with an Orion Research EA 940 pH meter that was calibrated with
85 three pH buffers (pH 4, pH 7, and pH 10). In solutions with an ionic strength higher than
86 0.10 m, hydrogen-ion concentrations on molar scale (pH) were determined from pH
87 readings by using correction factors (Rai et al., 1995). Based on the equation in
88 Xiong et al. (2010), pHs are converted to hydrogen-ion concentrations on molal scale
89 (pmH).

90 Solution samples were periodically withdrawn from experimental runs. Before
91 solution samples were taken, pH readings of experimental runs were first measured. The
92 sample size was usually 3 mL. After a solution sample was withdrawn from an
93 experiment and filtered with a 0.2 μm syringe filter, the filtered solution was then
94 weighed, acidified with 0.5 mL of concentrated TraceMetal[®] grade HNO₃ from Fisher
95 Scientific, and finally diluted to a volume of 10 mL with DI water. If subsequent
96 dilutions were needed, aliquots were taken from the first dilution samples for the second
97 dilution, and aliquots of the second dilution were then taken for the further dilution.

98 Boron concentrations of solutions were analyzed with a Perkin Elmer dual-view
99 inductively coupled plasma-atomic emission spectrometer (ICP-AES)
100 (Perkin Elmer DV 3300). Calibration blanks and standards were precisely matched with
101 experimental matrices. The linear correlation coefficients of calibration curves in all

102 measurements were better than 0.9995. The analytical precision for ICP-AES is better
103 than 1.00% in terms of the relative standard deviation (RSD) based on replicate analyses.

104

105 RESULTS

106 Experimental results are tabulated in Table 1. In Figure 1, solubilities of sodium
107 tetraborate as a function of experimental time are displayed. From Figure 1, it is clear
108 that steady-state concentrations are achieved in the first sampling, which was taken at 132
109 days (Table 1). It is assumed that steady-state concentrations represent equilibrium
110 concentrations, as the duration of experiments, up to 567 days, is significantly longer than
111 previous studies under similar conditions. For example, the equilibrium for the
112 quaternary $\text{Na}_2\text{B}_4\text{O}_7\text{—Na}_2\text{SO}_4\text{—K}_2\text{B}_4\text{O}_7\text{—K}_2\text{SO}_4\text{—H}_2\text{O}$ system at 15°C was attained in
113 3-7 days (Sang et al., 2011).

114 In Figure 2, concentrations of boron as a function of molalities of NaCl are
115 displayed. Figure 2 indicates that concentrations of boron in equilibrium with sodium
116 tetraborate have a strong dependence on concentrations of NaCl, with substantial
117 decrease in concentration of boron with increasing concentrations of NaCl. For instance,
118 the solubilities of sodium tetraborate are ~0.50 m in terms of total boron concentrations
119 in a 0.01 m NaCl solution, whereas the concentrations of boron decrease to ~0.15 m in a
120 5.0 m NaCl solution.

121

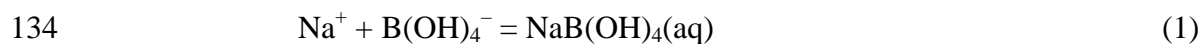
122 THERMODYNAMIC MODEL, DISCUSSIONS, AND APPLICATIONS

123 Felmy and Weare (1986) developed a thermodynamic model concerning borate in
124 the system $\text{Na—K—Ca—Mg—H—Cl—SO}_4\text{—CO}_2\text{—B(OH)}_4\text{—H}_2\text{O}$, based on literature

125 data. This model will be abbreviated as the FW86 model hereafter. Their model is an
126 extension of the Harvie et al. (1984) model to include borate species. In the
127 FW86 model, the species, $\text{NaB(OH)}_4(\text{aq})$, was not explicitly considered. However,
128 numerous researchers have suggested the existence of this complex in solutions
129 containing sodium (e.g., Reardon, 1976; Corti et al., 1980; Rowe et al., 1989; Pokrivski et
130 al., 1995; Akinfiiev et al., 2006). Therefore, this complex could be important in Na-rich
131 solutions.

132 In the work of Reardon (1976), the formation constants for the reaction,

133



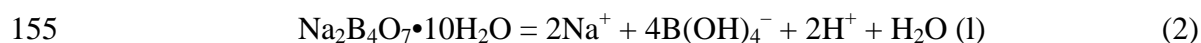
135

136 were determined in a NaCl medium with ionic strengths ranging from 0.165 m to
137 0.499 m at temperatures from 10 °C to 50 °C. To obtain the thermodynamic formation
138 constants at infinite dilution, Reardon (1976) used the activity coefficients of HCO_3^- and
139 $\text{H}_3\text{BO}_3(\text{aq})$ to approximate those of B(OH)_4^- and $\text{NaB(OH)}_4(\text{aq})$, respectively. The
140 thermodynamic formation constant at 25 °C for Reaction (1) obtained by Reardon (1976)
141 was 0.22 ± 0.10 .

142 In this study, conditional formation constants for Reaction (1) generated by
143 Reardon (1976) are re-evaluated by using the SIT model, following the methodology of
144 Grenthe et al. (1992). The $\log \beta_l$ at 25 °C obtained is 0.25 ± 0.01 (Figure 3 and Table 2).
145 Based on $\Delta\epsilon = -0.04 \pm 0.02$, the $\log \beta_l$ at 10 °C, 40 °C and 50 °C are also obtained
146 (Table 2). These values are in agreement with those of Pokrowski et al. (1995).

147 With the above $\log \beta_I$ for $\text{NaB(OH)}_4(\text{aq})$, experimental solubility data of borax in
148 NaCl produced in this study, and solubility data of borax in Na_2SO_4 from
149 Sborgi et al. (1924), are utilized to model the Pitzer parameters and $\log K_{sp}$ for borax with
150 the aid of the computer code EQ3/6 Version 8.0a (Wolery et al., 2010; Xiong, 2011).
151 The essence of the modeling is to minimize the difference between experimental and
152 model predicted values. The $\log K_{sp}$ for borax dissolution refers to the following
153 reaction,

154



156

157 In Figure 4, experimental data along with model predicted values are plotted. In
158 this plot, solubilities of $\text{Na}_2\text{B}_4\text{O}_7 \cdot 10\text{H}_2\text{O}$ in a Na_2SO_4 medium from Sborgi et al. (1924;
159 compiled in Linke, 1965, p. 826; and Silcock, 1979, Part 2, p. 582) are also included. It
160 should be mentioned that while the data of Sborgi et al. (1924) were tabulated in both of
161 the above compilations, Silcock (1979) cited an incorrect source. Notice that the values
162 predicted by the FW86 model are based on the parameters listed in Table 2. Similarly,
163 the values predicted by the model developed in this study are based on the parameters
164 tabulated in Table 3. It is clear from Figure 4 that the revised model developed in this
165 study performs very well in a wide range of ionic strength.

166 In Table 4, solution compositions of the assemblage of sodium tetraborate alone
167 or in equilibrium with other phases such as halite (NaCl), mirabilite ($\text{Na}_2\text{SO}_4 \cdot 10\text{H}_2\text{O}$),
168 and thenardite (Na_2SO_4), in mixtures of $\text{NaCl} + \text{Na}_2\text{SO}_4$ predicted by the revised model
169 and by the FW86 model are compared with independent experimental data from the

170 literature up to ionic strengths of 8.0 m, which are not used in model development in this
171 study. The experimental data are from Van't Hoff and Blasdale (1905; compiled in
172 Silcock, 1979) and Grushvitski and Flerinskava (1932; cited by Bukhshtein et al., 1953-
173 1954, and compiled in Silcock, 1979). The comparison demonstrates that while these
174 two models have similar precisions in prediction of concentrations of major ions, i.e.,
175 Na^+ , Cl^- , and SO_4^{2-} (Table 4), there is a significant improvement associated with the
176 current model in predicting solubilities of sodium tetraborate. The validation test
177 indicates that the differences between boron concentrations predicted by the current
178 model and experimental solubilities are less than 0.05 m with an error less than 25%
179 (Table 4 and Figure 5). In comparison, the differences between boron solubilities
180 predicted by the FW86 model and experimental solubilities are generally higher than 0.05
181 m, and can be as high as 0.17 m with an error up to 146%.

182 The revised model indicates that sodium tetraborate has solubilities much lower in
183 high ionic strength solutions in comparison with those predicted by the previous model.
184 This would have a wide range of implications. As an example, in the following, we
185 apply the current model to investigate the evolution of some boron-enriched brines in
186 China as a function of evaporation at 25°C.

187 The mildly alkaline brine in the Zhabei Salt Lake in Xizang (Tibet) Autonomous
188 Region, China, is enriched in boron (Gao et al., 2012) (Table 5). Similarly, as mentioned
189 in Introduction, the brine from the gas field in the western Sichuan Province, China, is
190 also enriched in boron (Table 6). Therefore, based on the thermodynamic model on
191 sodium tetraborate developed in this study, using EQ3/6 Version 8.0a, we can
192 quantitatively model by performing reaction path calculations the evolution of those

193 boron-enriched brines as a function of evaporation to provide insight into the potential
194 recovery of boron as sodium tetraborate via evaporation. In the reaction path
195 calculations, degrees of evaporation (DE) is defined as follows:

$$196 \quad DE = \left(1 - \frac{RMS}{OMS}\right) \times 100\% = \left(1 - \frac{RMS}{1000}\right) \times 100\% \quad (3)$$

197

198 where *RMS* is residual mass of solvent in grams, *OMS* is original mass of solvent. In the
199 reaction path calculations, *OMS* is scaled to 1000 grams of water.

200 In our reaction path calculations, the original aqueous solution masses for the
201 Zhabei Salt Lake and western Sichuan gas field brines are 1146 and 1433 grams,
202 respectively. As the original pH for the western Sichuan gas field brine was slightly
203 acidic (pH = 6.18), and borax will not precipitate, its pH was adjusted to 9.0 before
204 reaction path calculations. As the Zhabei Salt Lake brine is mildly alkaline, its pH was
205 not adjusted for reaction path calculations.

206 In Figure 6, amounts of mineral precipitated in mole are displayed as a function of
207 DE. From Figure 6, we can see that above DE 10, about 0.08 moles of borax will be
208 precipitated. Hydromagnesite (5424) [$Mg_5(CO_3)_4(OH)_2 \cdot 4H_2O$] (Xiong and Lord, 2008;
209 Xiong, 2011a) will also be precipitated. Trace amounts of calcite are also predicted to be
210 precipitated (Figure 6). In the evaporation experiments with the Zhabei Salt Lake brine
211 at 0°C performed by Gao et al. (2012), the precipitation of borax and magnesium
212 carbonate, possibly lansfordite ($MgCO_3 \cdot 5H_2O$), is also observed, based on phase
213 identifications using a polarizing microscope. However, it is worth noting that their
214 identification of lansfordite based on the optical method may not be exact. In fact,
215 studies on the sediments in the similar lakes in Xizang (Tibet) Autonomous Region have

216 indicated the presence of hydromagnesite (5424) instead of lansfordite (Goto et al.,
217 2003). Therefore, the magnesium carbonate identified by Gao et al. (2012) using the
218 optical method could be hydromagnesite (5424). In their evaporation experiments at 0°C,
219 Gao et al. (2012) did not mention the presence of calcite. This may be due to the
220 presence of calcite in trace amount, or the kinetics of calcite crystallization. In addition,
221 because of lower solubilities for salts at lower temperatures, mirabilite ($\text{Na}_2\text{SO}_4 \cdot 12\text{H}_2\text{O}$),
222 halite (NaCl), and sylvite (KCl) are also precipitated as major minerals in evaporation
223 experiments at 0°C of Gao et al. (2012). In contrast, because of undersaturation in
224 respect with mirabilite at 25°C, sulfate concentrations remain high during the evaporation
225 at 25°C (Figure 7A).

226 Evaporation of the brine from the gas field in the western Sichuan Province does
227 not precipitate borax and hydromagnesite (5424). Instead, halite, anhydrite (CaSO_4),
228 brucite [$\text{Mg}(\text{OH})_2$], magnesium chloride hydroxide hydrate (phase 5)
229 [$\text{Mg}_3\text{Cl}(\text{OH})_5 \cdot 4\text{H}_2\text{O}$] (Xiong et al., 2010), and sylvite are precipitated (Figure 6). Notice
230 that brucite is stable up to DE ~40. Above DE ~40, brucite is replaced by phase 5
231 (Figure 6). The absence of borax during evaporation of the brine from the western
232 Sichuan Province is due to the fact that the brine has higher magnesium concentrations
233 when the brine is chemically evolved (Figures 7A and 7B). In the evaporation
234 experiments with the brines having significant concentrations of magnesium and boron
235 performed by Gao and Li (1982) at temperatures from 16°C to 27°C, the precipitation of
236 borax is not observed neither because of high concentrations of magnesium. In our own
237 solubility experiments, we also observe that borax has much higher solubilities in
238 magnesium chloride solutions, which will be published later. In other words, the absence

239 of borax in the brine from the western Sichuan Province is well explained by the fact that
240 borax has higher solubilities in solutions with significant concentrations of magnesium.

241 In terms of chemical evolution of the brines induced by evaporation, the brine
242 from the Zhabei Salt Lake is dominated by Na-SO₄-Cl-B₄O₇ (Figure 7A), whereas the
243 brine from the western Sichuan Province is dominated by Na-K-Mg-Cl (Figure 7B).

244 The above reaction path calculations indicate that the brine from the Zhabei Salt
245 Lake is suitable for recovery of borax via evaporation at 25°C. The brine from the
246 western Sichuan Province is suitable for extraction of potassium as sylvite via
247 evaporation at 25°C.

248

249

250

251 SUMMARY

252 In this study, a thermodynamic model with high precision is developed for the
253 Na⁺-B(OH)₃-Cl⁻-SO₄²⁻ system, based on new experimental data. This model is
254 validated by independent experimental data in ternary mixtures of NaCl and Na₂SO₄.

255 With this model, solubilities of borax in concentrated NaCl, Na₂SO₄, and NaCl+Na₂SO₄
256 solutions can be accurately modeled.

257

258

259 ACNOWLEDGEMENTS

260 Sandia National Laboratories is a multiprogram laboratory operated by Sandia
261 Corporation, a wholly owned subsidiary of Lockheed Martin Corporation, for the United
262 States Department of Energy's National Nuclear Security Administration under Contract
263 DE-AC04-94AL85000. This research is funded by WIPP programs administered by the
264 Office of Environmental Management (EM) of the U.S Department of Energy. We are
265 grateful to Shelly Nielsen, Taya Olivas, Tana Saul, Diana Goulding, Brittany Hoard,
266 Cassandra Marrs, Danelle Morrill, Mathew Stroble, and Kira Vincent, for their laboratory
267 assistance. We thank the journal reviewers for their reviews, Dr. Rick Wilkin, the
268 Associate Editor, Dr. Keith Putirka, the Editor, for their reviews and editorial efforts.
269

270 REFERENCES

271

272 Akinfiev, N.N., Voronin, M.V., Zotov, A.V., Prokof'ev, V.Y. (2006) Experimental
273 investigation of the stability of a chloroborate complex and thermodynamic
274 description of aqueous species in the B-Na-Cl-O-H system up to 350°C.
275 *Geochemistry International*, 44, 867–878.

276 Borkowski, M., Richmann, M., Reed, D.T., and Xiong, Y.-L. (2010) Complexation of
277 Nd(III) with Tetraborate Ion and Its Effect on Actinide (III) Solubility in WIPP
278 Brine. *Radiochimica Acta*, 98, 577–582.

279 Bukshstein, V.M., Valyashko, M.G., and Pel'sh, A.D. (1953-1954) Spravochnik po
280 rastvorimosti solevykh system, A reference book of solubilities of salt systems
281 (Spravochnik po rastvorimosti solevykh system). Vol. I and II Izd. Vses. Nauch-
282 Issled. Inst. Goz., Goskhimizdat., Moscow-Leningrad.

283 Corti, H., Crovetto, R., and Fernandez-Prini, R. (1980) Mobilities and ion-pairing in
284 $\text{Li}(\text{OH})_4$ and $\text{NaB}(\text{OH})_4$ aqueous solutions. A conductivity study. *Journal of*
285 *Solution Chemistry*, 9, 617–625.

286 Felmy, A.R., and Weare, J.H. (1986) The prediction of borate mineral equilibria in
287 natural waters: Applications to Searles Lake, California. *Geochimica et*
288 *Cosmochimica Acta*, 50, 2771–2783.

289 Gao, F., Zheng, M.-P., Song, P.-S., Bu, L.-Z., Wang, Y.-S. (2012) The 273.15-K-
290 isothermal evaporation experiment of lithium brine from the Zhabei Salt Lake, Tibet,
291 and its geochemical significance. *Aquatic Geochemistry*, 18, 343–356.

292 Gao, S.-Y., and Li, G.-Y. (1982) The chemistry of borate in salt lake brine. Part One,
293 Behavior of borate during solar evaporation of brine (in Chinese with English
294 abstract). *Chemical Journal of Chinese Universities*, 3(2), 141–148.

295 Goto, A., Arakawa, H., Morinaga, H., and Sakiyama, T. (2003) The occurrence of
296 hydromagnesite in bottom sediments from Lake Siling, Central Tibet: implications
297 for the correlation among $\delta^{18}\text{O}$, $\delta^{13}\text{C}$ and particle density. *Journal of Asian Earth*
298 *Science*, 21, 979–988.

299 Grenthe, I., Fuger, J., Konings, R.J.M., Lemire, R.J., Muller, A.B., Nguyen-Trung. C.,
300 Wanner, H. (1992) *Chemical Thermodynamics of Uranium* New York: Elsevier
301 Science Publishers; 714 pp.

302 Grushvitski, V.E., and Flerinskava, E.M. (1932) Tr. Vses. Nauch.-Issled. Inst. Gal., cited
303 in Silcock, H. (1979) *Solubilities of Inorganic and Organic Compounds*, Volume 3,
304 Part 2, Page 585, Pergamon Press, New York.

- 305 Harvie, C.E., Møller, N., and Weare, J.H. (1984) The Prediction of Mineral Solubilities
306 in Natural Waters: The Na-K-Mg-Ca-H-Cl-SO₄-OH-HCO₃-CO₃-CO₂-H₂O System
307 to High Ionic Strengths at 25 °C. *Geochimica et Cosmochimica Acta*, 48, 723-751.
- 308 Lin, Y.-T., Yan, Y.-J., and Wu, Y.-L. (2000) Geochemical characteristics of gas field
309 water in one field in west Sichuan and its development evaluation (in Chinese).
310 *Natural Gas Industry (TIANRANQI GONGYE)*, 20, 9–14.
- 311 Linke, W.F. (1965) Solubilities of Inorganic and Metal-Organic Compounds, A
312 Compilation of Solubility Data from the Periodical Literature, Volume II, K-Z, 4th
313 Edition, American Chemical Society, Washington, D.C., 1914 pp.
- 314 Pokrovski, G.S., Schott, J., Sergeev, A.S. (1995) Experimental determination of the
315 stability constants of NaSO₄⁻ and NaB(OH)₄⁰ in hydrothermal solutions using a new
316 high-temperature sodium-selective glass electrode—Implications for boron isotopic
317 fractionation. *Chemical Geology*, 124, 253–265.
- 318 Rai, D., Felmy, A.R., Juracich, S.I., Rao, F.F. (1995) Estimating the Hydrogen Ion
319 Concentration in Concentrated NaCl and Na₂SO₄ Electrolytes. SAND94–1949
320 Sandia National Laboratories, Albuquerque, NM.
- 321 Reardon, E.J., (1976) Dissociation constants for alkali earth and sodium borate ion pairs
322 from 10 to 50 °C. *Chemical Geology*, 18, 309–325.
- 323 Rowe, L.M., Tran, L.B., and Atkinson, G., (1989) The effect of pressure on the
324 dissociation of boric acid and sodium borate ion pairs at 25 °C. *Journal of Solution*
325 *Chemistry*, 18, 675–689.
- 326 Sang, S.-H., Li, H., Sun, M.-L., Peng, J. (2011) Solid—liquid stable equilibria for the
327 quaternary Na₂B₄O₇—Na₂SO₄—K₂B₄O₇—K₂SO₄—H₂O system at 288 K. *Journal*
328 *of Chemical and Engineering Data*, 56, 1956–1959.
- 329 Sborgi, U., Bovalini, E., and Cappellini, L. (1924) Per lo stuio della doppia
330 decomposizione (NH₄)₂ + Na₂SO₄ ⇌ Na₂B₄O₇ + (NH₄)₂SO₄ in soluzione acqua.
331 Parte III. Sistema ternario Na₂B₄O₇, Na₂SO₄, H₂O. *Gazzetta chimica Italiana*, 54,
332 298–322.
- 333 Silcock, H. (1979) Solubilities of Inorganic and Organic Compounds, Volume 3,
334 Pergamon Press, New York.
- 335 U.S. DOE (1996) Compliance Certification Application 40 CFR Part 191 Subpart B and
336 C U.S. Department of Energy Waste Isolation Pilot Plant. Appendix SOTERM.
337 DOE/CAO 1996-2184. Carlsbad, NM: U.S. DOE Carlsbad Area Office.
- 338 Van't Hoff, I.H., and Blasdale, W.C. (1905) Examination on the formation conditions of
339 oceanic salt deposits. XLV. The occurrence of tincal and octaedric borax.

- 340 SITZUNGSBERICHTE DER KONIGLICH PREUSSISCHEN AKADEMIE DER
341 WISSENSCHAFTEN, 252, 1086–1090. Cited in Silcock, H., 1979. Solubilities of
342 Inorganic and Organic Compounds, Volume 3, Part 2, Page 584, Pergamon Press,
343 New York.
- 344 Wang, S.-A., Alekseev, E.V., Depmeier, W., and Albrecht-Schmitt, T.E. (2010)
345 Surprising coordination for plutonium in the first plutonium(III) borate. Inorganic
346 Chemistry, 50, 2079–2081.
- 347 Wang, S.-A., Alekseev, E.V., Depmeier, W., Albrecht-Schmitt, T.E. (2011) Recent
348 progress in actinide borate chemistry. Chemical Communications, 47, 10874–
349 10885.
- 350 Wolery, T.W., Xiong, Y.-L., and Long, J. (2010) Verification and Validation
351 Plan/Validation Document for EQ3/6 Version 8.0a for Actinide Chemistry,
352 Document Version 8.10. Carlsbad, NM: Sandia National laboratories. ERMS
353 550239.
- 354 Xiong, Y.-L. (2011a) Experimental determination of solubility constant of
355 hydromagnesite(5424) in NaCl solutions up to 4.4 m at room temperature.
356 Chemical Geology, 284, 262–269.
- 357 Xiong, Y.-L. (2011b) WIPP Verification and Validation Plan/Validation Document for
358 EQ3/6 Version 8.0a for Actinide Chemistry, Revision 1, Document Version 8.20.
359 Supersedes ERMS 550239. Carlsbad, NM. Sandia National Laboratories. ERMS
360 555358.
- 361 Xiong, Y.-L., and Lord, A.C.S. (2008) Experimental investigations of the reaction path
362 in the MgO–CO₂–H₂O system in solutions with ionic strengths, and their
363 applications to nuclear waste isolation. Applied Geochemistry, 23, 1634–1659.
- 364 Xiong, Y.-L., Deng, H.-R., Nemer, M., and Johnsen, S. (2010) Experimental
365 determination of the solubility constant for magnesium chloride hydroxide hydrate
366 (Mg₃Cl(OH)₅·4H₂O), phase 5) at room temperature, and its importance to nuclear
367 waste isolation in geological repositories in salt formations. Geochimica et
368 Cosmochimica Acta, 74, 4605–46011.
- 369
- 370

371
 372
 373

Table 1. Experimental results produced in this study at 22.5 ± 1.5 °C.

Experimental Number	Supporting Medium, NaCl, molal	Experimental time, days	pH	Molal total boron concentrations, $m_{\Sigma B}$, in equilibrium with sodium tetraborate
Na ₂ B ₄ O ₇ -NaCl-0.01-1	0.010	132	9.10	0.515
Na ₂ B ₄ O ₇ -NaCl-0.01-2	0.010	132	9.03	0.509
Na ₂ B ₄ O ₇ -NaCl-0.1-1	0.10	132	8.97	0.435
Na ₂ B ₄ O ₇ -NaCl-0.1-2	0.10	132	8.95	0.417
Na ₂ B ₄ O ₇ -NaCl-1.0-1	1.0	132	8.70	0.179
Na ₂ B ₄ O ₇ -NaCl-1.0-2	1.0	132	8.72	0.194
Na ₂ B ₄ O ₇ -NaCl-2.0-1	2.1	132	8.66	0.157
Na ₂ B ₄ O ₇ -NaCl-2.0-2	2.1	132	8.81	0.147
Na ₂ B ₄ O ₇ -NaCl-3.0-1	3.2	132	8.81	0.139
Na ₂ B ₄ O ₇ -NaCl-3.0-2	3.2	132	8.77	0.143
Na ₂ B ₄ O ₇ -NaCl-4.0-1	4.4	132	8.88	0.165
Na ₂ B ₄ O ₇ -NaCl-4.0-2	4.4	132	8.89	0.151
Na ₂ B ₄ O ₇ -NaCl-5.0-1	5.0	132	8.80	0.145
Na ₂ B ₄ O ₇ -NaCl-5.0-2	5.0	132	8.79	0.146
Na ₂ B ₄ O ₇ -NaCl-0.01-1	0.010	278	9.28	0.488
Na ₂ B ₄ O ₇ -NaCl-0.01-2	0.010	278	9.28	0.495
Na ₂ B ₄ O ₇ -NaCl-0.1-1	0.10	278	9.26	0.411
Na ₂ B ₄ O ₇ -NaCl-0.1-2	0.10	278	9.24	0.415
Na ₂ B ₄ O ₇ -NaCl-1.0-1	1.0	278	9.04	0.190
Na ₂ B ₄ O ₇ -NaCl-1.0-2	1.0	278	9.03	0.099
Na ₂ B ₄ O ₇ -NaCl-2.0-1	2.1	278	9.00	0.155
Na ₂ B ₄ O ₇ -NaCl-2.0-2	2.1	278	8.98	0.152
Na ₂ B ₄ O ₇ -NaCl-3.0-1	3.2	278	8.96	0.143
Na ₂ B ₄ O ₇ -NaCl-3.0-2	3.2	278	8.93	0.140
Na ₂ B ₄ O ₇ -NaCl-4.0-1	4.4	278	9.06	0.139
Na ₂ B ₄ O ₇ -NaCl-4.0-2	4.4	278	9.05	0.142
Na ₂ B ₄ O ₇ -NaCl-5.0-1	5.0	278	8.96	0.141
Na ₂ B ₄ O ₇ -NaCl-5.0-2	5.0	278	8.96	0.142
Na ₂ B ₄ O ₇ -NaCl-0.01-1	0.010	327	9.33	0.482
Na ₂ B ₄ O ₇ -NaCl-0.01-2	0.010	327	9.28	0.508
Na ₂ B ₄ O ₇ -NaCl-0.1-1	0.10	327	9.26	0.436

Na ₂ B ₄ O ₇ -NaCl-0.1-2	0.10	327	9.22	0.430
Na ₂ B ₄ O ₇ -NaCl-1.0-1	1.0	327	9.09	0.207
Na ₂ B ₄ O ₇ -NaCl-1.0-2	1.0	327	9.10	0.210
Na ₂ B ₄ O ₇ -NaCl-2.0-1	2.1	327	8.99	0.160
Na ₂ B ₄ O ₇ -NaCl-2.0-2	2.1	327	9.00	0.161
Na ₂ B ₄ O ₇ -NaCl-3.0-1	3.2	327	9.00	0.151
Na ₂ B ₄ O ₇ -NaCl-3.0-2	3.2	327	8.95	0.157
Na ₂ B ₄ O ₇ -NaCl-4.0-1	4.4	327	9.10	0.151
Na ₂ B ₄ O ₇ -NaCl-4.0-2	4.4	327	9.11	0.147
Na ₂ B ₄ O ₇ -NaCl-5.0-1	5.0	327	8.97	0.151
Na ₂ B ₄ O ₇ -NaCl-5.0-2	5.0	327	9.01	0.158
Na ₂ B ₄ O ₇ -NaCl-0.01-1	0.010	377	9.39	0.513
Na ₂ B ₄ O ₇ -NaCl-0.01-2	0.010	377	9.38	0.509
Na ₂ B ₄ O ₇ -NaCl-0.1-1	0.10	377	9.32	0.468
Na ₂ B ₄ O ₇ -NaCl-0.1-2	0.10	377	9.33	0.482
Na ₂ B ₄ O ₇ -NaCl-1.0-1	1.0	377	9.09	0.214
Na ₂ B ₄ O ₇ -NaCl-1.0-2	1.0	377	9.09	0.231
Na ₂ B ₄ O ₇ -NaCl-2.0-1	2.1	377	9.03	0.168
Na ₂ B ₄ O ₇ -NaCl-2.0-2	2.1	377	9.03	0.171
Na ₂ B ₄ O ₇ -NaCl-3.0-1	3.2	377	9.01	0.153
Na ₂ B ₄ O ₇ -NaCl-3.0-2	3.2	377	9.00	0.149
Na ₂ B ₄ O ₇ -NaCl-4.0-1	4.4	377	9.08	0.152
Na ₂ B ₄ O ₇ -NaCl-4.0-2	4.4	377	9.09	0.146
Na ₂ B ₄ O ₇ -NaCl-5.0-1	5.0	377	9.00	0.152
Na ₂ B ₄ O ₇ -NaCl-5.0-2	5.0	377	9.02	0.149
Na ₂ B ₄ O ₇ -NaCl-0.01-1	0.010	425	9.35	0.514
Na ₂ B ₄ O ₇ -NaCl-0.01-2	0.010	425	9.31	0.532
Na ₂ B ₄ O ₇ -NaCl-0.1-1	0.10	425	9.26	0.531
Na ₂ B ₄ O ₇ -NaCl-0.1-2	0.10	425	9.25	0.458
Na ₂ B ₄ O ₇ -NaCl-1.0-1	1.0	425	9.04	0.221
Na ₂ B ₄ O ₇ -NaCl-1.0-2	1.0	425	9.03	0.222
Na ₂ B ₄ O ₇ -NaCl-2.0-1	2.1	425	8.96	0.171
Na ₂ B ₄ O ₇ -NaCl-2.0-2	2.1	425	8.97	0.171
Na ₂ B ₄ O ₇ -NaCl-3.0-1	3.2	425	8.95	0.161
Na ₂ B ₄ O ₇ -NaCl-3.0-2	3.2	425	8.93	0.156
Na ₂ B ₄ O ₇ -NaCl-4.0-1	4.4	425	9.02	0.158
Na ₂ B ₄ O ₇ -NaCl-4.0-2	4.4	425	9.04	0.154
Na ₂ B ₄ O ₇ -NaCl-5.0-1	5.0	425	8.96	0.159

Na ₂ B ₄ O ₇ -NaCl-5.0-2	5.0	425	8.97	0.162
Na ₂ B ₄ O ₇ -NaCl-0.01-1	0.010	567	9.28	0.489
Na ₂ B ₄ O ₇ -NaCl-0.01-2	0.010	567	9.28	0.497
Na ₂ B ₄ O ₇ -NaCl-0.1-1	0.10	567	9.24	0.429
Na ₂ B ₄ O ₇ -NaCl-0.1-2	0.10	567	9.23	0.426
Na ₂ B ₄ O ₇ -NaCl-1.0-1	1.0	567	9.00	0.199
Na ₂ B ₄ O ₇ -NaCl-1.0-2	1.0	567	9.00	0.203
Na ₂ B ₄ O ₇ -NaCl-2.0-1	2.1	567	8.94	0.157
Na ₂ B ₄ O ₇ -NaCl-2.0-2	2.1	567	8.94	0.167
Na ₂ B ₄ O ₇ -NaCl-3.0-1	3.2	567	8.93	0.160
Na ₂ B ₄ O ₇ -NaCl-3.0-1R	3.2	567	8.92	0.155
Na ₂ B ₄ O ₇ -NaCl-3.0-2	3.2	567	8.90	0.154
Na ₂ B ₄ O ₇ -NaCl-4.0-1	4.4	567	8.99	0.148
Na ₂ B ₄ O ₇ -NaCl-4.0-2	4.4	567	9.01	0.152
Na ₂ B ₄ O ₇ -NaCl-5.0-1	5.0	567	8.93	0.158
Na ₂ B ₄ O ₇ -NaCl-5.0-2	5.0	567	8.93	0.154

374
375

376

377 Table 2. Felmy and Weare (1986) model for the Na–B(OH)₃–Cl–SO₄ system

Pitzer Binary Interaction Coefficients				
Species, <i>i</i>	Species, <i>j</i>	$\beta^{(0)}$	$\beta^{(1)}$	C^ϕ
Na ⁺	B(OH) ₄ ⁻	-0.0427	0.089	0.0114
Na ⁺	B ₃ O ₃ (OH) ₄ ⁻	-0.056	-0.910	
Na ⁺	B ₄ O ₅ (OH) ₄ ²⁻	-0.11	-0.40	
Pitzer Mixing Parameters and Interaction Parameters Involving Neutral Species				
Species, <i>i</i>	Species, <i>j</i>	Species, <i>k</i>	θ_{ij} or λ_{ij}	Ψ_{ijk} or ζ_{ijk}
B(OH) ₄ ⁻	Cl ⁻	Na ⁺	-0.065	-0.0073
B(OH) ₄ ⁻	SO ₄ ⁻²		-0.012	
B ₃ O ₃ (OH) ₄ ⁻	Cl ⁻	Na ⁺	0.12	-0.024
B ₃ O ₃ (OH) ₄ ⁻	SO ₄ ⁻²		0.10	
B ₄ O ₅ (OH) ₄ ⁻²	Cl ⁻	Na ⁺	0.074	0.026
B ₄ O ₅ (OH) ₄ ⁻²	SO ₄ ⁻²		0.12	
B(OH) ₃ (aq)	Cl ⁻		0.091	
B(OH) ₃ (aq)	SO ₄ ⁻²	Na ⁺	0.018	0.046
B(OH) ₃ (aq)	B ₃ O ₃ (OH) ₄ ⁻		-0.20	
B(OH) ₃ (aq)	Na ⁺		-0.097	
Equilibrium Constant for Solubility Reaction				
Reaction			log K	
Na ₂ B ₄ O ₇ •10H ₂ O = 2Na ⁺ + 4B(OH) ₄ ⁻ + 2H ⁺ + H ₂ O			-24.49	

378

379

380
 381
 382

Table 3. The revised thermodynamic model for the Na–B(OH)₃–Cl–SO₄ system developed in this study*.

Pitzer Mixing Parameters and Interaction Parameters Involving Neutral Species				
Species, <i>i</i>	Species, <i>j</i>	Species, <i>k</i>	θ_{ij} or λ_{ij}	Ψ_{ijk} or ζ_{ijk}
B(OH) ₄ ⁻	SO ₄ ⁻²		0.17 ± 0.03	
NaB(OH) ₄ (aq)	Na ⁺		0.093 ± 0.005	
B ₄ O ₅ (OH) ₄ ⁻²	SO ₄ ⁻²	Na ⁺		0.1 ± 0.2
Equilibrium Constants for Solubility and Complex Formation Reactions				
Reaction			log <i>K</i> or log β _l at 25 °C unless otherwise noted	
Na ₂ B ₄ O ₇ •10H ₂ O = 2Na ⁺ + 4B(OH) ₄ ⁻ + 2H ⁺ + H ₂ O			-24.80 ± 0.10 (2σ)	
Na ⁺ + B(OH) ₄ ⁻ = NaB(OH) ₄ (aq)			0.29 ± 0.01 (10 °C) 0.25 ± 0.01 (25 °C) with Δε = -0.04 ± 0.02 0.24 ± 0.01 (40 °C) 0.26 ± 0.02 (50 °C)	

383 *Unless otherwise noted, other parameters, which are not listed, are the same as those in
 384 Felmy and Weare (1986) model.
 385

386 Table 4. Comparison of independent, experimental equilibrium compositions for
 387 multiple equilibrium assemblages containing sodium tetraborate ($\text{Na}_2\text{B}_4\text{O}_7 \cdot 10\text{H}_2\text{O}$)
 388 (borax) with predicted compositions in mixtures of NaCl and Na_2SO_4 at 25 °C

Experimental data for equilibrium compositions					
m_{Na}	m_{Cl}	m_{SO_4}	$m_{\Sigma\text{B}}$	Equilibrium Assemblage*	References
6.967	5.516	0.694	0.125	BRX+HLT+THNDT	Van't Hoff and Blasdale (1905)
6.355	5.925	0.183	0.128	BRX+HLT	Grushvitski and Flerinskava (1932)
6.527	5.408	0.526	0.134	BRX+HLT	<i>ibid.</i>
6.716	5.286	0.673	0.167	BRX+HLT	<i>ibid.</i>
6.939	5.441	0.716	0.132	BRX+HLT+THNDT	<i>ibid.</i>
6.603	4.723	0.903	0.149	BRX	<i>ibid.</i>
6.477	3.168	1.619	0.141	BRX+MRBLT+THNDT	<i>ibid.</i>
3.774	0.248	1.734	0.117	BRX+MRBLT	<i>ibid.</i>
Equilibrium compositions predicted by the Felmy and Weare (1986) model					
m_{Na}	m_{Cl}	m_{SO_4}	$m_{\Sigma\text{B}}$	Equilibrium Assemblage*	
6.971	5.484	0.691	0.212	BRX+HLT+THNDT	
6.364	5.896	0.182	0.206	BRX+HLT	
6.532	5.381	0.523	0.209	BRX+HLT	
6.704	5.260	0.670	0.211	BRX+HLT	
6.943	5.413	0.712	0.212	BRX+HLT+THNDT	
6.602	4.699	0.898	0.214	BRX	
6.367	3.229	1.512	0.229	BRX+MRBLT+THNDT	
3.833	0.246	1.721	0.289	BRX+MRBLT	
Equilibrium compositions predicted by the model developed in this study					
m_{Na}	m_{Cl}	m_{SO_4}	$m_{\Sigma\text{B}}$	Equilibrium Assemblage*	
6.947	5.494	0.692	0.136	BRX+HLT+THNDT	
6.347	5.906	0.183	0.151	BRX+HLT	
6.512	5.393	0.524	0.141	BRX+HLT	
6.683	5.272	0.671	0.137	BRX+HLT	
6.922	5.426	0.714	0.136	BRX+HLT+THNDT	
6.577	4.711	0.900	0.131	BRX	
6.284	3.273	1.475	0.120	BRX+MRBLT+THNDT	
3.780	0.247	1.728	0.151	BRX+MRBLT	
Difference in %** between experimental values and those predicted by the FW86 model					
ΔNa in %	ΔCl in %	ΔSO_4 in %	$\Delta\Sigma\text{B}$ in %	Equilibrium Assemblage*	

0.060	-0.586	-0.507	69.788	BRX+HLT+THNDT
0.133	-0.483	-0.482	60.851	BRX+HLT
0.084	-0.496	-0.497	55.925	BRX+HLT
-0.170	-0.504	-0.503	26.362	BRX+HLT
0.072	-0.508	-0.507	60.305	BRX+HLT+THNDT
-0.016	-0.514	-0.515	43.776	BRX
-1.701	1.941	-6.656	62.343	BRX+MRBLT+THNDT
1.555	-0.725	-0.725	145.848	BRX+MRBLT
Difference in %** between experimental values and those predicted by the model developed in this study				
ΔNa in %	ΔCl in %	ΔSO_4 in %	ΔSB in %	Equilibrium Assemblage*
-0.290	-0.402	-0.274	9.240	BRX+HLT+THNDT
-0.121	-0.309	-0.308	18.448	BRX+HLT
-0.227	-0.284	-0.285	5.249	BRX+HLT
-0.495	-0.275	-0.274	-18.006	BRX+HLT
-0.245	-0.273	-0.272	2.587	BRX+HLT+THNDT
-0.392	-0.259	-0.260	-11.967	BRX
-2.974	3.327	-8.884	-14.637	BRX+MRBLT+THNDT
0.145	-0.307	-0.307	28.758	BRX+MRBLT

389 *Abbreviations for minerals: BRX, borax ($\text{Na}_2\text{B}_4\text{O}_7 \cdot 10\text{H}_2\text{O}$); HLT, halite (NaCl);
 390 MRBLT, mirabilite ($\text{Na}_2\text{SO}_4 \cdot 10\text{H}_2\text{O}$); THNDT, thenardite (Na_2SO_4).
 391 **Difference in % is defined as, using concentrations of sodium on molal scale as an
 392 example,

$$393 \quad \Delta\text{Na in \%} = 100 \times \frac{m_{\text{Na, Model}} - m_{\text{Na, Experimental}}}{m_{\text{Na, Experimental}}}$$

394

395

396 Table 5. Chemical composition of the brine from the Zhabei Salt Lake, Xizang (Tibet)
 397 Autonomous Region, China (from Gao et al., 2012)
 398

Composition	Na ⁺	K ⁺	Ca ²⁺	Mg ²⁺	Cl ⁻	ΣCO ₃	SO ₄ ²⁻	B ₄ O ₇ ²⁻
mol•kg ⁻¹	0.738	0.0660	0.00203	0.188	0.404	0.124	0.933	0.0864
Other parameters	pH		Density, g/cm ³			Total Dissolved Salts, mg/L		
Value	9.19		1.046			61,740		

399 *Original compositions are converted to molal concentrations by this work, based on
 400 density and total dissolved salts.

401
 402
 403
 404
 405
 406
 407
 408
 409

Table 6. Chemical composition of the brine from the western Sichuan gas field, China
 (from Lin et al., 2000)*

Composition	Na ⁺	K ⁺	Ca ²⁺	Mg ²⁺	Cl ⁻	ΣCO ₃	SO ₄ ²⁻	B ₄ O ₇ ²⁻
mol•kg ⁻¹	4.90	1.59	0.105	0.152	6.90	0.0215	0.0169	0.0184
Other parameters	pH		Density, g/cm ³			Total Dissolved Salts, mg/L		
Value	6.18		1.2359			377,270		

410 *Original compositions are converted to molal concentrations by this work, based on
 411 density and total dissolved salts.

412
 413

414 Figure Captions

415

416 Figure 1. A plot showing experimental total boron concentrations in equilibrium with
417 sodium tetraborate produced in this study as a function of experimental time.

418

419

420 Figure 2. A plot showing experimental total boron concentrations in equilibrium with
421 sodium tetraborate produced in this study as a function of molalities of NaCl.

422

423

424 Figure 3. A plot showing $[\log \beta_1^f + 2D]$ as a function of ionic strengths, where
425 $\log \beta_1^f$ denotes conditional formation constants of $\text{NaB(OH)}_4(\text{aq})$ at certain ionic strengths
426 from Reardon (1976).

427

428

429 Figure 4. A plot showing a comparison of experimental total boron concentrations in
430 equilibrium with sodium tetraborate in NaCl and Na_2SO_4 solutions with predicted total
431 boron concentrations as a function of ionic strengths.

432

433

434 Figure 5. A plot showing differences in total boron concentrations in equilibrium with
435 sodium tetraborate between experimental and predicted values in $\text{NaCl} + \text{Na}_2\text{SO}_4$
436 solutions as a function of ionic strengths.

437

438

439 Figure 6. A plot showing mineral precipitation as a function of degree of evaporation
440 (DE).

441

442

443 Figure 7. A plot showing chemical evolution of the brine as a function of degree of
444 evaporation (DE). A. the brine from the Zhabei Salt Lake, China; B. the brine from the
445 western Sichuan Province, China

446

